# Classical RFID Versus Chipless RFID Read Range: Is Linearity a Friend or a Foe?

Nicolas Barbot, Olivier Rance, Etienne Perret

# Classical RFID vs. Chipless RFID Read Range: Is Linearity a Friend or a Foe?

Nicolas Barbot, *Member, IEEE,* Olivier Rance, *Member, IEEE,* and Etienne Perret, *Senior Member, IEEE*

***Abstract*—This paper presents a comparison between the read range of classical RFID and chipless RFID in free space and real environments. From the presented model, read range is derived using analytical formulation over non-isolated channels for both technologies. The paper shows that the well known bounds classically used in free space cannot be achieved in real environments i.e., subjected to leakage, coupling and/or reflections) and therefore need to be modified. Although the introduced bound for semi-passive tags is close to the one corresponding to free space, we show however that for chipless tags read range can not be predicted by the radar equation and presents severe limitations since these tags are linear time-invariant systems. This new bound does not depend on the transmitted power nor the reader sensitivity but relies on the concept of residual environment. We show that, this quantity is the key parameter to evaluate the read range of a chipless RFID system. Moreover, the residual environment can easily be estimated or measured for any reading system. We show that the proposed bound can accurately predict the read range of a chipless system in different environments from anechoic chamber to non-stationary real environments. Results are confirmed in simulation and measurements where difference between theoretical read range and the measured one is only 20 cm.**

***Index Terms*—Chipless RFID, linear time-invariant system, radar cross-section, read range, RFID.**

## I. Introduction

RFID technology gathers classical RFID (*i.e.*, with a chip) and chipless RFID. Classical RFID (passive and semi-passive) is a mature technology which has been developed, optimized and integrated for decades [1]–[3] whereas chipless RFID has been introduced lately [4]–[7] mainly to reduce the cost of the tags. Also, a lot of efforts have been placed in chipless, on both tag and reader design, to close the gap between these two technologies. However, performance in term of coding capacity and read range still largely benefits to classical RFID.

Read range is maybe the most important metric since numerous applications directly rely on this parameter. Also, classical models used to determine read range for both technologies only consider free space propagation. Moreover, as we will see, the theory predicts similar read range in free space for semi-passive and chipless technologies. However, in real environments *i.e.,* over channels subjected to leakage, coupling and/or reflections, both technologies are characterized by very different read range. On one side, passive and semi-passive tags can be read at distances higher than dozens of meters by industrial (low-cost) readers. On the other side, chipless tags are limited to dozens of centimeters even when they are read by (expensive) laboratory equipment. The objective of the paper is to highlight the fundamental difference between classical and chipless RFID technologies by investigating the impact of the linearity over the achievable read range. The paper introduces a consistent model to predict the read range in real environments for both technologies with analytical expressions. These bounds are different of the ones obtained in free space and greatly depend on the technology.

The rest of the paper is organized as follows: Section II presents a study on the read range of classical and chipless RFID in free space. Detailed state of the art is also presented at the end of this section. Section III presents the difference between classical RFID and chipless RFID and introduces new bounds for both technologies in real environments. Section IV presents the results corresponding to the bound for the chipless technology in both simulation and measurements. Finally, Section V gives new approaches to break the limitation introduced and explored in Section III and Section IV for the chipless technology.

The authors are with Univ. Grenoble Alpes, Grenoble INP, LCIS, F-26000 Valence, France.

## II. Free Space Channel

Classical RFID and chipless RFID share a lot of common properties. They both have similar Radar Cross-Section (RCS) and are affected by comparable path loss. However both technologies also exhibit some differences, such as activation power and modulation loss. This section presents a fair comparison between classical and chipless RFID for a dipole scatterer in free space.

Reading distance of both techniques can be computed analytically in free space. For passive RFID, read range is mainly limited by the power received by the tag. On the other side, for semi-passive RFID tags (*i.e.*, tags assisted by a battery) and for chipless tags, read range depends on the received power received at the reader side. For passive tags, the received power, assuming a perfect matching, can be obtained using Friis equation [8]:

$$P_{rt} = P_t G_t G \left(\frac{\lambda}{4\pi d}\right)^2 \tag{1}$$

where $P_t \cdot G_t$ is the Effective Isotropic Radiated Power (EIRP) of the reader, $G$ is the tag antenna gain and $d$ the distance between the reader and the tag. Also, passive tags can only operate if the received power is higher than the chip sensitivity $P_{rt\,min}$ which corresponds to the minimal power permitting to activate the chip. This value lies typically in-between $-10$ dBm (100 µW) for old chips (*e.g.*, Impinj Monza 2), to $-18$ dBm (16 µW) for new chips (*e.g.*, Impinj Monza 5). On the other side, semi-passive and chipless tags are not affected

by the activation power and can operate whatever the received power. In these cases, read range is limited by the power received by the reader which depends on the RCS of the tag. For minimum scattering antennas (like the dipole antenna), the scalar RCS value $\sigma$ depends on the impedance of the load and can be simply expressed as [1]:

$$\sigma = \frac{\lambda^2 G^2 R_a^2}{\pi |Z_a + Z_l|^2} \tag{2}$$

where $Z_a$ and $Z_l$ are the impedances of the antenna and the load respectively. This RCS is maximum for short circuit load and minimum (and equal to 0) for open circuit load. Note that this formula is valid for both chipped and chipless tags. Power received by the reader is obtained using the classical radar equation [9]:

$$P_{rr} = \frac{P_t G_t G_r \lambda^2 \sigma}{(4\pi)^3 d^4} \tag{3}$$

Note that (3) is valid in free space and does not take into account the leakage, the coupling and/or the reflections over different objects. Finally, read range can be determined by finding the distance at which (3) is lower than the reader sensitivity $P_{rr\,min}$. For dipole scatterer, read range is maximum when the dipole is short-circuited. On the other side, for semi-passive RFID, read range is only limited by the state of the higher RCS value since, even if the other state is associated to a received power lower than $P_{rr\,min}$, the received signal can still be decoded. Thus, in free space environment (and assuming a perfect isolation), semi-passive tags and chipless tags are characterized by the exact same RCS and consequently, the same read range.

For comparison purposes, we consider in the following, that the reader has the same performance for both technologies with an emission power of $P_t = 4$ W EIRP (with $G_t = G_r = 1$), and a sensitivity of $P_{rr\,min} = -80$ dBm. For both tags, a $\lambda/2$ dipole antenna operating at 915 MHz has been considered with a gain of 2.15 dBi and a RCS given by (2). Note that, due the low bandwidth of the ISM band, the chipless tag should probably be composed of a single resonator and could encode a single bit of information (0 or 1) if standards-compliance is required. However, this low coding capacity does not impact the results on the read range presented here. For passive tag, sensitivity has been set to $-18$ dBm and modulation loss at $-6$ dB (which corresponds to a commutation between matched and open states). For semi-passive tags, switching can be realized between open and short states. Results are presented in Fig. 1 for the frequency of 915 MHz. This simple study shows that the theoretical distance at which a passive tag could be read is 17 m in free space. On the other side, read range of a semi-active tag and chipless tag is 38 m. Note that these results are theoretical and valid only in free space and correspond to the maximal read range that can be achieved by each systems.

A lot of RFID transponders have been proposed in the literature to reach these two bounds. Fig. 2 presents the maximal read range of passive and semi-passive as a function of the EIRP for a frequency of 915 MHz for passive tags [2], [3], [10]–[14] (see blue squares in Fig. 2), semi-passive tags [11], [15]–[18] (see red triangles in Fig. 2) and chipless tags [6], [7],

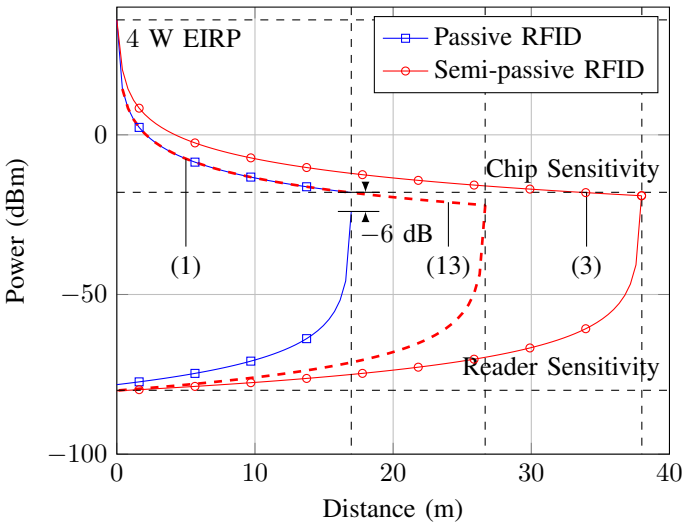


Fig. 1. Received power in free space as a function of the distance for passive, semi-passive at 915 MHz. Chipless RFID performance is identical to semi-passive RFID in free space. Dashed line corresponds to (13).

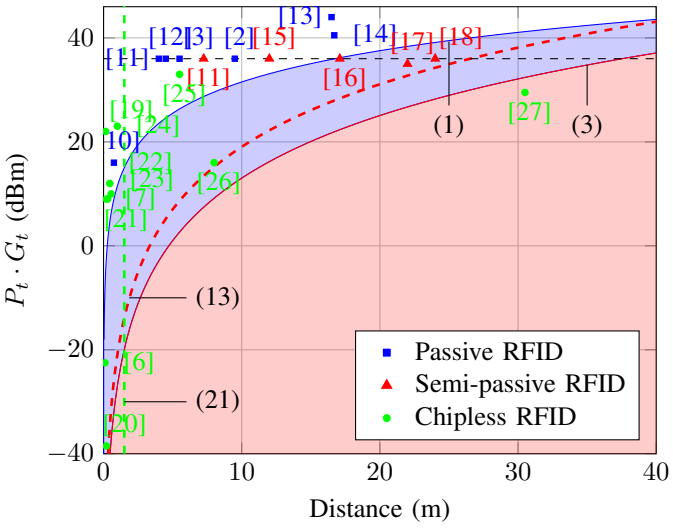


Fig. 2. Theoretical read range vs. EIRP for passive, semi-passive at 915 MHz in free space and their associated measured read range. Chipless RFID performance is identical to semi-passive RFID in free space. Dashed lines correspond to (13) and (21).

[19]–[29] (see green points in Fig. 2). Note that, for a given frequency, semi-passive tags and chipless tags are bounded by the same maximal read range [see (3)] but the bound presented in red is an upper bound for chipless tags since their frequency of operation is usually higher than 915 MHz. We can see that classical (passive and semi-passive) RFID tags achieve a large part of the theoretical read range. For example, measured read range with passive tag in [14] is 16.7 m for a theoretical value of 28 m which corresponds to 59% of the theoretical read range. Also, authors in [18] achieve a distance of 24 m for semi-passive tags which represents 64% of the theoretical read range. However, for chipless RFID, (and except for [25]–[29] which use very directive antennas), measured read range is always lower than 1 m. Also, read range is comparable even if reader architecture is very different. For example, authors

in [6] achieve a read range of 10 cm using an expensive Vector Network Analyzer (VNA) (frequency domain) whereas authors in [20] reach a distance 20 cm using a homemade low-cost reader (time domain). Finally and more importantly, read range in chipless RFID is not increased when the transmitted power is increased. For example, in [19], authors use an EIRP of 22 dBm at 915 MHz which corresponds to a theoretical read range of 16 m however measured read range is 15 cm which is less than 1% of the theoretical read range in free space.

Based on these observations, the objective of the paper is to understand the fundamental difference in read range between classical RFID and chipless RFID. Moreover, when theoretical read range of chipless RFID is investigated in the literature, maximal distance is systematically extracted from (3), see for example [23], [24], [26], [30]–[32]. This paper shows that even if this bound is valid in free space for semi-passive and chipless RFID, read range in real environments is degraded for both technologies. The paper provides also demonstration and analytical expressions valid in real environments in each case. For the chipless technology, the bound is based on the concept of residual environment which is the key parameter to evaluate the read range of any chipless RFID system. These results will permit to increase the comprehension of the inherent limitations of chipless RFID and also open the way to new techniques allowing to increase the read range of chipless RFID by a factor of 50 in very specific conditions.

## III. Non-Isolated Channels

Read ranges obtained form (1) and (3) for passive RFID and, semi-passive and chipless RFID respectively, are valid in free space. Also, the latter configuration assumes a perfect isolation between the transmitting and the receiving antenna and that no reflection are present inside the environment (*i.e.*, that the received power is only due to the RCS of the object). However, in real environments, a fraction of the emitted signal, possibly distorted, is received by the receiver due to leakage, coupling or reflections over different objects present inside the environment. These channels are called in the following, non-isolated channels and gathers multiple cases from anechoic chamber to complex indoor environments. For these channels, results presented in Section II do not hold anymore and significantly depend on the considered technology. Finally, the impact on the read range is presented in each case, for classical and chipless RFID systems. It should also be noted that, obviously, the equations derived subsequently lead to lower read range than those obtained in Section II.

### A. Classical RFID

If a Continuous Wave (CW) $x(t)$ is impinging a passive or semi-passive tag and if the power available at the chip is higher than its sensitivity, the load variation $m(t)$ realized by the chip actually modifies the backscattered signal by the tag in time domain which can be expressed, without loss of generality, as:

$$y(t) = af(x(t), m(t)) + x(t) * e(t) \tag{4}$$

where $a$ corresponds to the round trip path loss between the antennas and the tag, $f()$ is a function corresponding to the backscattered modulation done by the tag and $e(t)$ is the impulse response of the environment seen by the antennas (which takes into account leakage, coupling, and/or reflections). Note that, in this model, the environment is a linear time-invariant system. Assuming narrowband signal and replacing $x(t)$ by its expression, (4) can be rewritten:

$$y(t) = aA_R(t)\cos(2\pi f_0 t + \phi_R(t)) + A_e\cos(2\pi f_0 t + \phi_e) \tag{5}$$

where $A_R(t)$ and $\phi_R(t)$ are respectively the instantaneous amplitude and phase of the modulated signal produced by the tag. Note that this decomposition is not limited to RFID but is valid for all modulated signals. On the other side $A_e$ and $\phi_e$ are the attenuation and phase shift of the environment due to leakage, coupling and/or reflections. (Details on the second term will be highlighted in the next subsection.) Note that $A_e$ and $\phi_e$ do not depend on time.

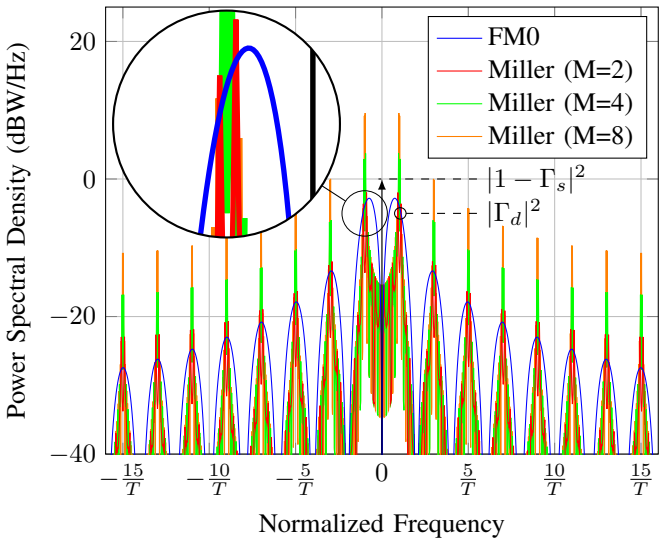


Fig. 3. Power spectral density of the signal backscattered by the tag when a CW is used by the reader.

Since data sent back by the tag to the reader are random, the backscattered signal is a stochastic process. Assuming the stationnarity in the wide sense, its Power Spectral Density (PSD) can be defined:

$$S_Y(f - f_0) = a^2 S_R(f - f_0) + |A_e|^2\delta(f - f_0) \tag{6}$$

The exact characteristics of its PSD, however depends on the data encoding used by the tag. The UHF RFID standard [33] defines two different modulations for the tag which are FM0 and Miller (with different subcarriers sequences). Analytical formula of the PSD for FM0 is known and is equal to the Manchester encoding [34]. For Miller modulation, analytical formula is also known, but without considering the subcarrier sequences [35]. Fig. 3 presents the PSD of the different modulations used by the tag for power wave reflection coefficient $\Gamma_{1,2} = \pm 1$. PSD of FM0 has been obtained using the analytical formula, for Miller modulations, results have been obtained by averaging the Fourier transform of the autocorrelation function of a randomly modulated signal [36]. Note that curves are centered around 0 Hz since they correspond to the baseband

signals, real signals are centered around $f_0$. Also, according to the RFID standard, the backscatter link frequency $1/T$ and can range from 40 kHz to 640 kHz.

From [37], this modulated signal can always be decomposed into a static part and a dynamic part:

$$\begin{aligned} S_Y(f-f_0) &= a^2[S_{R_s}\delta(f-f_0) + S_{R_d}(f-f_0)] \\ &\quad + |A_e|^2\delta(f-f_0) \qquad (7) \\ &= [a^2 S_{R_s} + |A_e|^2]\delta(f-f_0) \\ &\quad + a^2 S_{R_d}(f-f_0) \qquad (8) \end{aligned}$$

where $S_{R_s}$ and $S_{R_d}(f-f_0)$ correspond to the static and differential part respectively. Also, since the contribution of the environment (leakage, coupling and reflections) is a linear time-invariant system, the corresponding reflected power is only located at $f_0$ when the reader uses a CW. After the demodulation, a classical RFID reader uses a high pass filter to remove the static component due to the environment and (a part of) the backscattered signal from the tag [38]:

$$S_{Y_{hp}}(f) = a^2 S_{R_d}(f) \qquad (9)$$

This signal can be successfully decoded if the power corresponding to $Y_{hp}(f)$ is higher than the threshold of the reader:

$$\begin{aligned} P_{Y_{hp}} &= \int_{-b}^{+b} a^2 S_{R_d}(f)\,\mathrm{d}f \geq \int_{-b}^{+b} N_0\,\mathrm{d}f \qquad (10) \\ &= \frac{P_t G_t G_r \lambda^2 \sigma_d}{(4\pi)^3 d^4} \geq P_{rr\,min} \qquad (11) \end{aligned}$$

where $b$ is the (single sided) bandwidth of the reader, $N_0$ is the PSD of the additive white gaussian noise and $P_{rr\,min} = 2N_0 b$ is the minimum power which can be detected by the reader. Note that the path loss $a^2$ generally depends on the complex summation of the backscattered signal plus the different reflections of the environment. The transition from (10) to (11) assumes that the round trip attenuation between the antennas and the tag is the same as the one in free space. Also $\sigma_d$ is the differential RCS defined in [37] as:

$$\sigma_d = \frac{\lambda^2 G^2}{4\pi}\frac{|\Gamma_1 - \Gamma_2|^2}{4} \qquad (12)$$

Note that this definition corresponds to $1/4$ of the classical differential RCS introduced in [39] to satisfy the law of energy conservation. From (11), isolating $d$ leads to:

$$d_{sp} \leq \sqrt[4]{\frac{P_t G_t G_r \lambda^2 \sigma_d}{(4\pi)^3 P_{rr\,min}}} \qquad (13)$$

Note that (13) is valid in real environments and can be seen as a modified radar equation [whose classical form is given by (3) and is valid only in free space]. This distance does not depend on the higher RCS value [as in (3)] but on the differential RCS of the tag due to the high pass filter used by the reader. Also, it is important to notice that the read range in real environments obtained with (13) is reduced compared to the one used in free space with (3), since $\sigma_d$ is at least four times lower than $\sigma$. This bound is presented in Fig. 1 and Fig. 2 in dashed line.

Finally, since the PSD of a modulating tag has been obtained by sending a CW toward the tag (which contains a power

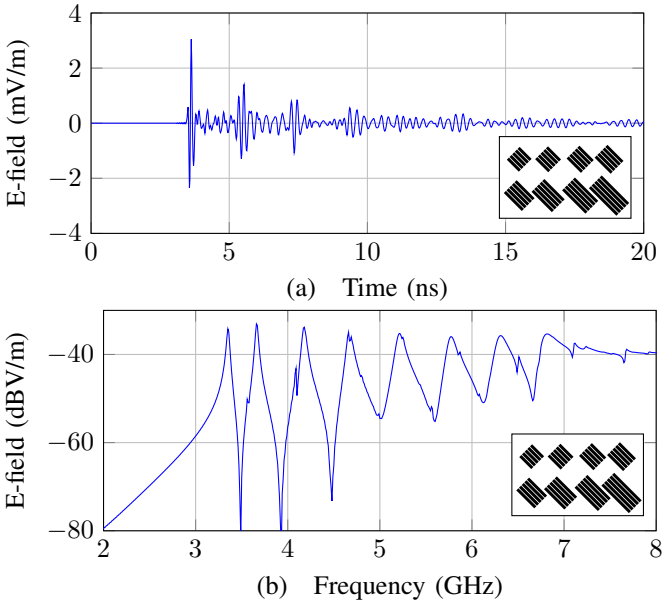


Fig. 4. Backscattered E-field in (a) time domain impulse response, (b) frequency domain function transfer of the chipless tag introduced in [7].

only at $f = f_0$), it means that the modulated power has been spread at $f \neq f_0$. Thus, the modulation of the chip breaks the linearity property. In that sense, a classical RFID tag can not be modeled as a linear time-invariant system. Also, note that if the tag is not activated (no modulation), tag becomes a simple linear time-invariant system like any other object in the environment.

### B. Chipless RFID

A chipless tag can usually encode information in time domain (by using reflections along a transmission line) or in frequency domain (by using multiples resonators). We assume in the following, that the chipless tag uses the frequency domain to encode information (but the same conclusions can be drawn with time domain tags or any other chipless tag).

Frequency domain chipless tags are composed of multiples scatterers where each scatterer is a resonating structure whose resonant frequency is linked to its geometrical dimensions. In order to interrogate a tag, a reader sends a UWB signal toward the tag and measures the backscattered response to estimate the resonant frequencies. The signal sent by the reader could be an harmonic sweep (like VNA-based measurement [6]) a pulse (train) [20], or a (modulated) white noise [19]. Fig. 4 presents the backscattered signal of the tag introduced in [7] in cross-polarization in time and frequency domain. Response has been obtained using the temporal solver of CST. Simulation uses a 0.08 ns gaussian pulse and a farfield probe which has been placed at a distance of 1 m of the tag. Frequency response is computed using a FFT on the time domain backscattered signal. We can see that the response of the tag in frequency domain presents eight peaks which correspond to the eight resonators. Moreover, note that to read the tag ID, the transmitted pulse bandwidth has to cover the entire band used by the tag.

Also, since a chipless tag is a linear time-invariant system, results presented in Fig. 4 can be interpreted as the impulse response $h(t)$ (in time) or transfer function $H(f)$ (in frequency) if the pulse used tends to a Dirac function $\delta(t)$. Note that, a single quantity, *i.e.*, the impulse response or the transfer function allows to fully characterize the tag whatever the input signal used by the reader. Also, if this chipless tag (or any linear time-invariant system), is exited by a CW at frequency $f_0$, the received signal can be expressed as:

$$y(t) = |H(f_0)| \cos(2\pi f_0 t + \text{Arg}(H(f_0))) \tag{14}$$

which is also an harmonic function at the same frequency $f_0$ with an attenuation $|H(f_0)|$ and phase shift of $\text{Arg}(H(f_0))$. Finally, due to the linearity, we can see that a chipless tag can only backscatter a signal in the same and exact bandwidth that the one used by the reader. This linearity constitutes a fundamental difference compared to semi-passive RFID and directly affects the read range of chipless tags in real environments.

Read range obtained from (3) does not hold for chipless RFID (or any linear time-invariant system) in environment other than (perfectly isolated) free space. To understand this idea, let's assume that we send a pulse $x(t)$ with a power spectral density of $|X(f)|^2$ toward the tag, in an environment which reflects and possibly distorts a fraction of the emitted signal. In reception, the received signal can be written:

$$y_{tot}(t) = x(t) * [ah(t) + e_1(t)] \tag{15}$$

where $a$ represents the same path loss as the one defined in (4). Also $e_1(t)$ is the impulse response of the environment seen by the antennas and takes into account leakage, coupling and/or reflections over different objects. Note that $h(t)$ and $e_1(t)$ are both linear time-invariant systems. Also, the power associated with the second term is usually significantly higher that the one received from the tag. For compensating the environment, a second measurement without the tag is needed:

$$y_e(t) = x(t) * e_2(t) \tag{16}$$

where $e_2(t)$ is the impulse response of the environment without the tag. Note that $e_1(t)$ and $e_2(t)$ are generally not identical possibly due to a modification of the environment between the two measurements, and/or due to the coupling between the tag and the antenna (or any other surrounding object). The response of the tag is obtained by subtracting the measurement of the tag with the environment (15) and the measurement without the tag (16):

$$y(t) = ax(t) * h(t) + x(t) * [e_1(t) - e_2(t)] \tag{17}$$

Note that $e_1(t) - e_2(t)$ is defined in the following, as the impulse response of the residual environment. This quantity is mainly linked to the modification of the environment seen by the antennas during the two measurements. Taking the Fourier transform of (17) to obtain the frequency domain signal leads to:

$$Y(f) = aX(f) \cdot H(f) + X(f) \cdot [E_1(f) - E_2(f)] \tag{18}$$

In practice, PSD associated to $|X(f) \cdot [E_1(f) - E_2(f)]|^2$ is significantly higher than the reader sensitivity (linked to the noise floor of the instrument). Also, since both tag and residual environment are linear time-invariant systems, increasing the pulse energy allows to increase the energy backscattered by the tag but also from the residual environment with the exact same proportion.

Maximal reading distance of a chipless tag can be extracted by finding the distance $d$ where the power spectral density received from the tag is higher than the one received from the residual environment:

$$|aX(f) \cdot H(f)|^2 \geq |X(f) \cdot [E_1(f) - E_2(f)]|^2 \tag{19}$$

Simplifying and recognizing the expression of the RCS of the tag $\sigma(f)$ and the transfer function of the residual environment (noted $\epsilon(f)$):

$$\frac{G_t G_r \lambda^2 \sigma(f)}{(4\pi)^3 d^4} \geq |\epsilon(f)|^2 \tag{20}$$

Also, (20) uses the same approximation as (11) *i.e.*, that the path loss between the tag and the antenna is equal to the one in free space. Isolating $d$ leads to:

$$d_c \leq \sqrt[4]{\frac{G_t G_r \lambda^2 \sigma(f)}{(4\pi)^3 |\epsilon(f)|^2}} \tag{21}$$

Note that, contrary to the read range extracted from (3), this expression does not depend on the the transmitted power nor the sensitivity of the reader and is generally much lower than the one given by (3). Also, this expression is valid for all channels where perfect isolation between emitter and receiver cannot be maintained *i.e.*, channels subjected to leakage, coupling and/or reflections which is the case for all real environments from anechoic chamber to non-stationnary indoor environments. Moreover, (21) allows to clearly separate the contribution of the tag *i.e.*, $\sigma(f)$ and the contribution of the residual environment *i.e.*, $|\epsilon(f)|^2$ on the read range of the chipless tag. Finally, (21) remains valid even if post-processing techniques (*e.g.* time gating) are applied on the received signal (only $\sigma(f)$ and $|\epsilon(f)|^2$ need to be estimated for the considered technique). This bound has been reported in Fig. 2 (green dashed line) for a dipole scatterer and a residual environment of $-60$ dB at a frequency of $915$ MHz (and corresponds to an upper bound since classical chipless tags generally operate at higher frequencies).

## IV. Results

This section highlights the impact of the linearity over the performance of the chipless technology in both simulation and measurement.

### A. Impact of the Transmitted Power

As we have seen, chipless tags are linear time-invariant systems, as such, they presents the same behavior than any other object inside the environment. Also, as predicted by (21) transmitted power can not help to improve the decoding performance. Fig. 5 presents the simulated results of the tag introduced in [7]. This chipless tag uses a $0.8$ mm Rogers RO4003C substrate with a ground plane. A metallic plate, with the same dimension and rotated by an angle of $45°$, has

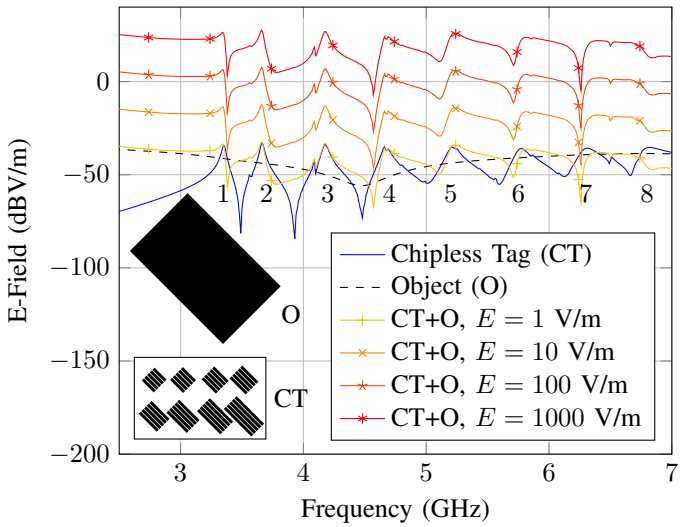


Fig. 5. Response of a chipless tag and a metallic object for different power in simulation.

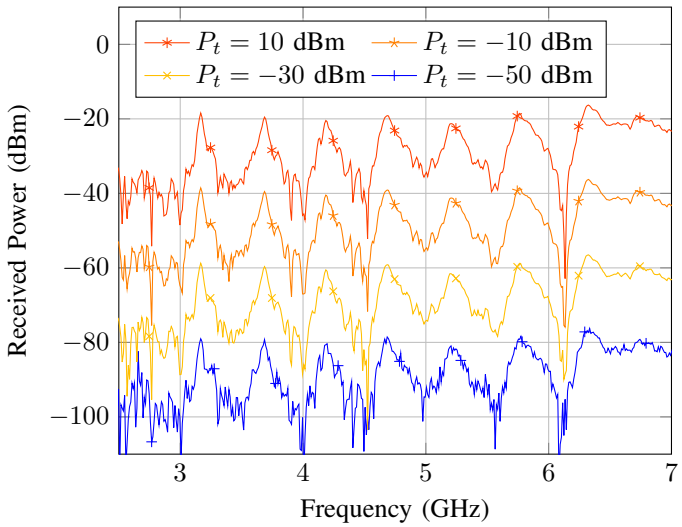


Fig. 6. Received power in cross-polarization with the tag introduced in [7] as a function of the transmitted power.

also been placed near the tag. A vertical plane wave is used as excitation and the received field is measured in reflection with a farfield probe at a distance of 1 m. We can see that the magnitude of the E-field at the resonant frequencies is around $-35$ dBV/m for all resonators. Moreover the response of the object presents a magnitude which is close to the chipless tag for low and high frequencies and a minimum for 4.3 GHz. Thus, the total response of both tag and object, which corresponds to the complex summation of the E-fields, presents clear peaks in the middle of the band (*i.e.*, resonators 2, 3, 4 and 5) since the object response lower than the tag response. On the other side, peaks cannot be clearly identified when magnitude of the object is higher or equal to the tag response (*i.e.*, resonators 1, 6, 7 and 8). Simulations have also been done for different electric field values. Results show that if the electric field value is multiplied by 10, the received field is also multiplied by 10 which shifts the curve by an offset of 20 dB. Note that the increase affects both the tag response and the object response since both structures are linear time-invariant systems. Finally, we can see that the tag response (and consequently the chipless tag read range) could not be improved by increasing the transmitted power.

Results presented in Fig. 5 have been obtained from simulation and do not take into account the additive noise associated with real measurements. Fig. 6 extends these results by presenting the same tag [7] measured in real environment at a distance of 20 cm. Measurements have been done with a dual-access dual-polarization Satimo QH2000 antenna connected to respectively port 1 and receiver B of port 2 of Agilent N5222A VNA. Note that the curves do not correspond to the $S_{21}$ parameter anymore since the received signal is not divided by the reference R but is instead directly proportional to the received power. Results show that we can read the tag almost independently of the transmitted power *i.e.*, from 10 dBm (maximal output power of the VNA) to $-40$ dBm. For these powers, the variation of the signal compared to the simulation (see Fig. 5) are not due to noise but to the residual environment. On the other side, at $-50$ dBm, received power is just above the noise floor of the instrument (which was measured at $-90$ dBm) and perturbations are, in this case, dominated by noise (which affects differently the received power). Thus, as far as the transmitted power is higher that $-50$ dBm, same conclusions can be drawn as in the simulation (see Fig. 5), and read range cannot be increased by increasing the transmitted power.

### *B. Estimation of the Residual Environment*

As it has been shown in Section III, read range of chipless RFID system is directly linked to the transfer function of the residual environment $\epsilon(f)$. Thus, estimating this quantity for different readers, post-processing techniques and/or environments is essential to understand the performance of a chipless RFID system.

For frequency domain readers, $|\epsilon(f)|^2$ can be computed by:

$$|\epsilon(f)|^2 = \frac{|Y_{e_1}(f) - Y_{e_2}(f)|^2}{|X(f)|^2} \tag{22}$$

where $X(f)$ is the transmitted pulse spectrum and $Y_{e_1}(f)$ and $Y_{e_2}(f)$ are the received signals of two measurements without the tag. Also, if the instrument allows to estimate the S-parameters (*e.g.*, a VNA), which are ratioed quantities between the reflected and incident wave, the residual environment can simply be expressed as:

$$|\epsilon(f)|^2 = |S_{YXe_1} - S_{YXe_2}|^2 \tag{23}$$

where $S_{YXe_n}$ are two measurements of the S-parameter without the tag.

For time domain readers, $|\epsilon(f)|^2$ can be computed by:

$$|\epsilon(f)|^2 = \frac{\left|\int_{-\infty}^{+\infty}[y_{e_1}(t) - y_{e_2}(t)]e^{-2j\pi ft}\mathrm{d}t\right|^2}{\left|\int_{-\infty}^{+\infty} x(t)e^{-2j\pi ft}\mathrm{d}t\right|^2} \tag{24}$$

where $x(t)$ is the transmitted pulse and $y_{e_1}(t)$ and $y_{e_2}(t)$ are two received signals of the environment without the tag. Note

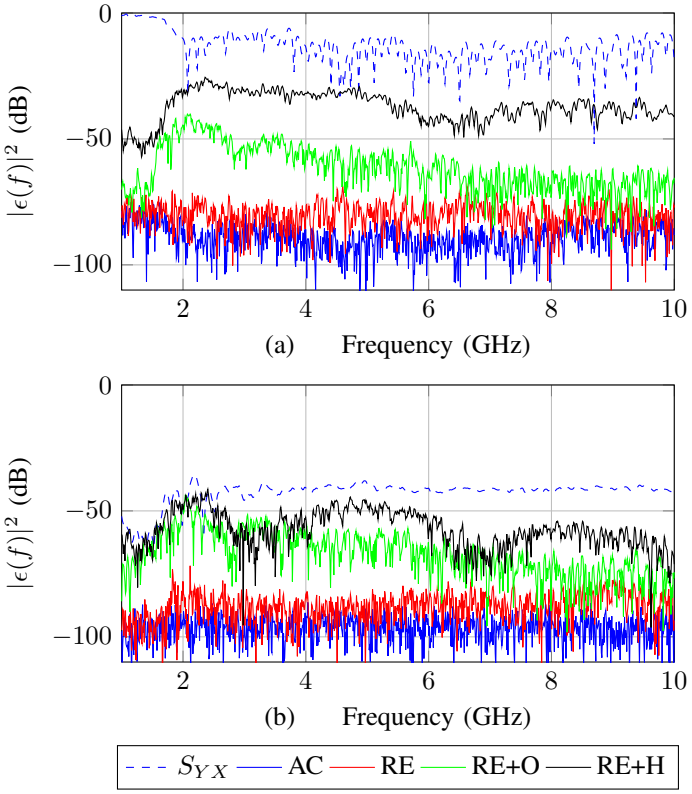


Fig. 7. Different residual environments obtained in anechoic chamber (AC), real environment (RE), real environment with moving objects (RE+O) and real environment with the hand in front of the antenna (RE+H) in (a) co-polarization and (b) in cross-polarization.

TABLE I
AVERAGE RESIDUAL ENVIRONMENT $|\epsilon(f)|^2$ OF DIFFERENT OBJECTS MEASURED AT A DISTANCE OF 20 CM WITH A VNA BASED READER

| Objects | Co-polarization | Cross-polarization |
|---|---|---|
| Empty | $-82$ dB | $-81$ dB |
| Paperclip | $-46$ dB | $-55$ dB |
| 1$ coin | $-40$ dB | $-62$ dB |
| Hand | $-37$ dB | $-48$ dB |
| Empty packaging | $-48$ dB | $-56$ dB |
| Operator at 1 m | $-55$ dB | $-57$ dB |

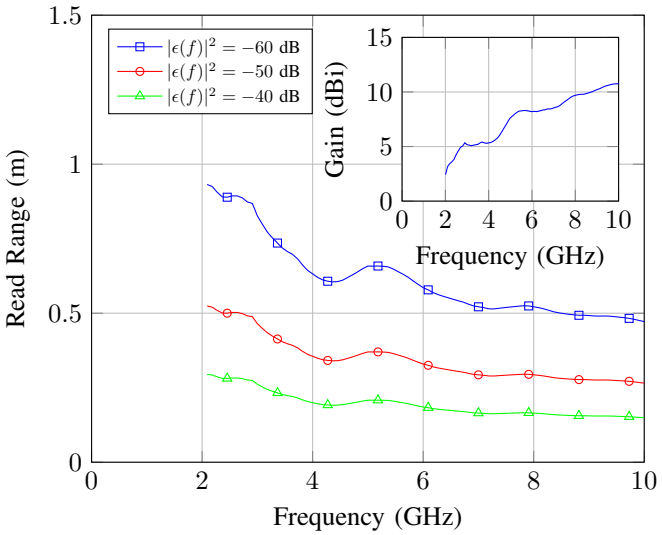


Fig. 8. Read range obtained from (21) for different values of $|\epsilon(f)|^2$ considering the RCS of the dipole antenna loaded by a short-circuit. Inset: Satimo QH2000 gain as a function of the frequency.

that (22), (23) and (24) do not take into account the residual environment linked to the coupling between the tag and the environment.

Fig. 7 presents the residual environment obtained from a VNA-based reader and compares the performance of co-polarization and cross-polarization reading methods for an IF bandwidth of 1 kHz for both configurations. We can see that, although $S_{11}$ (*i.e.*, co-polarization) and $S_{21}$ (*i.e.*, cross-polarization) differ by more than 20 dB, their associated residual environment anechoic chamber are relatively close around $-90$ dB. Note that this result corresponds to the lowest residual environment which can be measured by the instrument. Also, in this case, residual environment is limited by the noise floor of the instrument (which was also measured around $-90$ dBm). In real environment, we can observe a slight degradation for both polarizations with a residual environment around $-80$ dB for co-polarization and cross-polarization. Moreover, when dynamic environment is considered (by moving some objects in the antenna vicinity), both methods presents the same degradation (note that to provide a fair comparison, the same objects has been moved identically for both configurations). However, when the hand is placed in front the antenna at the same distance of 20 cm, we can see that cross-polarization presents a lower residual environment compared to co-polarization. Thus, as shown by (21), for a given tag, read range in cross-polarization is expected to be higher than co-polarization in real applications (when the tag held by the user hand for example).

Finally, Table I presents the average residual environment of different objects measured at a distance of 20 cm by a VNA between 3 and 8 GHz. In anechoic environemnt, the average residual environment could be as low as $-80$ dB however, when objects are added or moved, residual environment can be drastically increased even by slight modification or variation of the environment. For example the simple presence of a paperclip adds a contribution of 36 dB in co-polarization and 26 dB in cross-polarization. Also, measuring a tag by holding it with the hand adds a contribution higher than 30 dB which can be more important than the response of the tag itself. These results directly affect the read range of the chipless system.

### C. Read Range Evaluation

Read range achieved by a chipless tag in real environment can be determined by (21) and depends mainly on the tag RCS $\sigma(f)$ and $|\epsilon(f)|^2$. Fig. 8 presents the predicted read range of a dipole scatterer with $\sigma = G^2\lambda^2/\pi$, read in co-polarization and for different values of $|\epsilon(f)|^2$. The considered antenna is a Satimo QH2000 whose gain values have been measured using a MVG Starlab. We can see that this bound provides a read range which is significantly lower than the one obtained with (3). For example, at a frequency of 915 MHz, read range

predicted by (3) is 38 m (see Fig. 1 and 2) whereas the one predicted by (21) is lower than 1 m for a residual environment corresponding to a real environment *i.e.*, $|\epsilon(f)|^2 = -50$ dB). We also see that the bound is a decreasing function of the frequency since the RCS of a dipole antenna also decrease with the wavelength. Finally, read range in chipless RFID is limited by the level of the residual environment. For example, in co-polarization, when the tag is held by the hand, the residual environment is equal to $-40$ dB (see Table I), thus the read range of the dipole scatterer can not exceed 20 cm.

As said previously, (21) remains valid when post-processing techniques are applied by the chipless reader. The following study presents the performance gain which can be achieved using time gating operation using simulation. Note that performance of different techniques (*e.g.*, short time-Fourier transform) can also be analyzed with a similar approach. We consider the configuration presented in Fig. 5 where the chipless tag (CT) and an additional object (O) can be read independently. Note that, in real measurements, tag and object responses are superimposed in the frequency domain. Time gating is applied on the time domain signals to separate the contribution of the object and the tag. The method depends on 3 parameters which are the starting time $T_{\text{start}}$, stopping time $T_{\text{stop}}$ and the window function (*i.e.* rectangular). The performance mainly depends on the starting time which allows to reduce the impact of the objects (*i.e.* residual environment $|\epsilon(f)|^2$) while preserving the energy associated to the tag (*i.e.*, $\sigma(f)$. Fig. 9(a) presents the evolution of the power of both $|\epsilon(f)|^2$ (*i.e.,* O) and $\sigma(f)$ (*i.e.,* CT) for the different resonant frequencies as a function of the starting time. Note that since frequency response $|\epsilon(f)|^2$ is flat in frequency (see Fig. 5), the residual environment has a limited support in time. Thus, $|\epsilon(f)|^2$ in Fig 9(a) does not depend on the resonant frequency (*i.e.*, all curves are superimposed). On the other side, $\sigma(f)$ strongly depends on the resonant frequency. Also, the slope of the curves is slower for low frequency resonators since they are associated to higher quality factors.

These 2 quantities $\sigma(f)$ and $|\epsilon(f)|^2$ can now be re-injected into (21) to find the maximum read range as a function of $T_{\text{start}}$. Results are presented in Fig. 9(b) for the eight resonators. We can see that time gating is more effective for low frequency resonators since contributions are easily separated in the time domain. For high frequency resonators, support of the tag response and object response are overlapped and time gating performance is reduced. Also, we can see that the optimization of $T_{\text{start}}$ value can increase the read range of the chipless tag form 20 cm to 30 cm for this specific environment.

A study of the coding capacity can also be conducted from Fig. 9. Indeed, through this figure, it is possible to illustrate the dependence that exists between the read range and the coding capacity. At a given distance, coding capacity is proportional to the number of resonator which can be read *i.e.*, whose distance to the reader antenna is lower than their read range. When the tag is placed at 10 cm, the 8 resonators can be read without time gating thus the tag capacity, at this distance, is maximum and equal to 18.5 bits [7]. For a distance of 25 cm, only 4 resonators can be read without time gating which corresponds to a coding capacity of 9.25 bits. Thus we can clearly see that

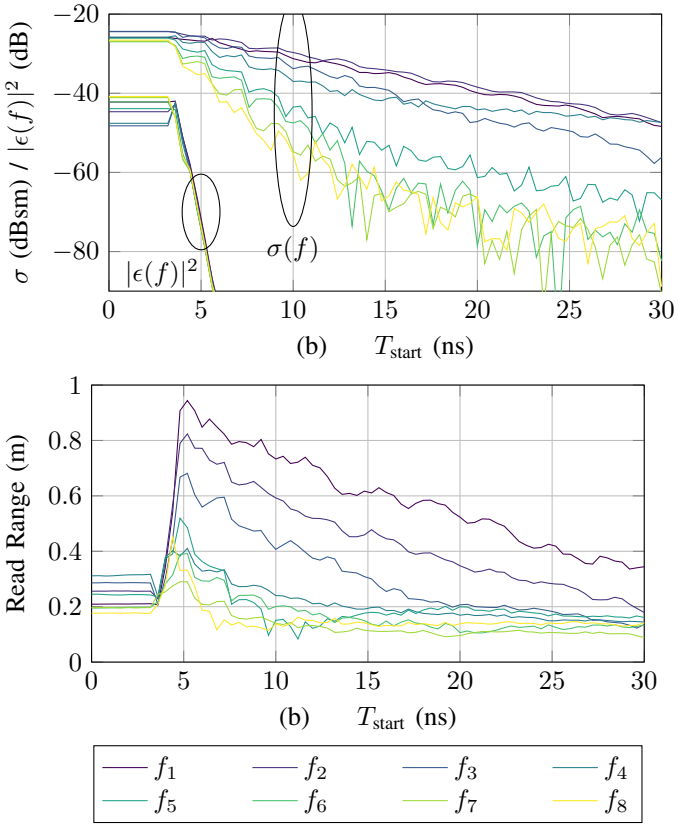


Fig. 9. (a) Residual environment $|\epsilon(f)|^2$ and RCS $\sigma(f)$ as a function of the starting time. (b) Read range obtained with (21) as a function of the starting time.

a trade-off exists in-between coding capacity and read range for LTI systems.

The final study presents the read range of classical chipless resonators *i.e.*, C-shape, rectangular loop and dipoles with ground plane [7]. Dimensions are given in Fig. 10. In order to determine the RCS of each scatterer, simulation has been performed to estimate the magnitude of the peak as a function of the resonator length $l$. Results are presented in Fig. 11 where we can see that the RCS peak value (red dashed curve) decreases as the function of the frequency for all resonators. Moreover RCS of the loop resonator is higher than 6 dB compared to the C-shape one (RCS of the dipole in cross-polarization is in-between these to values). This information can now be used to determine the read range of each tag by using (21) (when reading is done by a Satimo QH2000). Results are plotted in Fig. 12, measurements in real environment are also presented with dot markers for all the resonators. Non Line Of Sight (LOS) results have also been added by measuring the read range of tag introduced in [7] through a 1 cm thickness phenolic resin laminate plate ($\epsilon = 5.6$) characterized by an average power transmission coefficient of $-2.6$ dB. Theoretical read range in non LOS configuration have been obtained by using (21) and by taking the additional (round trip) attenuation through the material. Note that measured read ranges have been obtained using a single empty measurement and without using post-processing technique. Also, the proposed read range accurately predicts

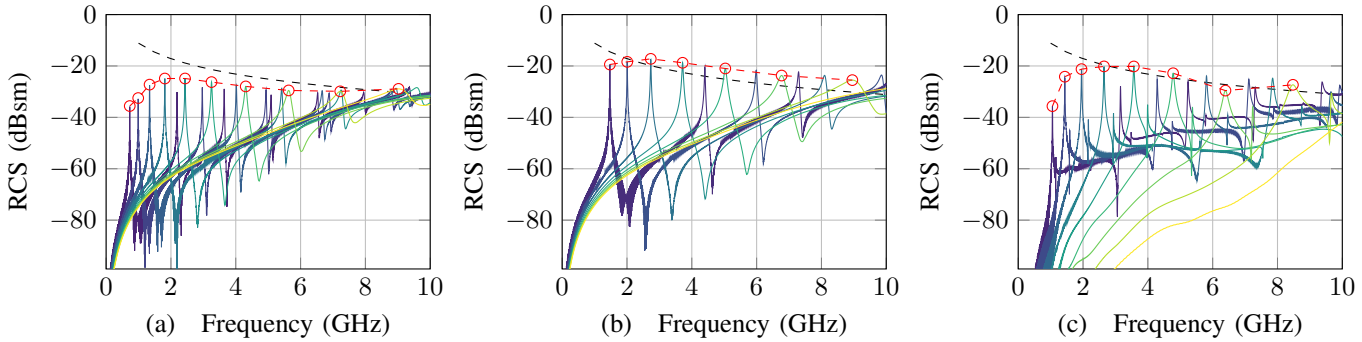


Fig. 10. Radar cross section of classical chipless resonators for different length $l$ (a) C-shape in co-polarization, (b) rectangular loop in co-polarization and (c) 45° dipoles in cross-polarization [7]. Red dashed curve presents the maximum of the RCS value as a function of the frequency. Black dashed curve is the theoretical RCS of a short circuit dipole antenna in co-polarization [see (2)].

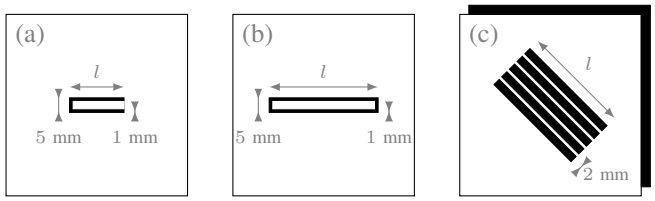


Fig. 11. Resonators used in the study: (a) C-shape resonator, (b) rectangular loop and (c) dipoles with ground plane. Resonator length $l$ varies form 4 to 79 mm. All resonators use a 0.8 mm Rogers RO4003C substrate.

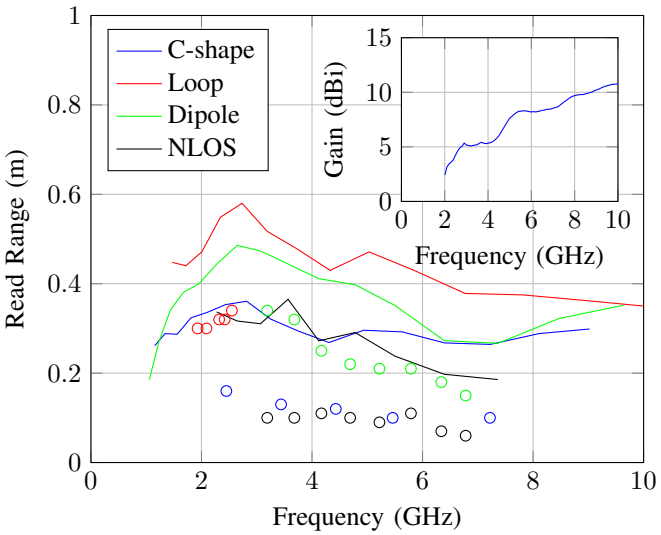


Fig. 12. Read range of classical chipless resonators obtained from (21) for a residual environment of $|\epsilon(f)|^2 = -50$ dB and considering Satimo QH2000 antenna. Marks correspond to the measured read range for the corresponding resonators. Inset: Satimo QH2000 gain as a function of the frequency.

the measured ones for all resonators and at all frequencies with a difference lower than 20 cm even in non LOS environment. Note that, difference can be explained by the structural mode of the tag itself and the coupling with other object in the tag's vicinity which also increase the residual environment.

## V. Perspectives

The impact of the linearity over the chipless technology has largely been underestimated. In fact, chipless RFID is the only case of data transmission based on linear time-invariant transponders (which makes this technology very different compared to classical communication systems *e.g.*, RFID). This property has also two direct consequences over the characteristics of any chipless tag. First, it ensures to reduce the cost of the tag which can be as low as 0.4 cent [40] since no modulation (or non-linear effect) is effectively realized by the tag. Almost all chipless applications require and rely on this cost. Second, and due to this same linearity property, a chipless tag has also the same behavior as any other object present inside the environment. As we have seen, this result places severe limitations on the read range of the chipless RFID technology which can not be compensated by increasing the transmitted power or the sensitivity of the reader. It is important to note that these two consequences are closely related and can not be easily separated for most of the chipless tag designs. Nevertheless, read range can be increased by breaking the linearity property. In this specific case read range is extracted from the modified radar equation [see (13)]. This bound depends on the transmitted power and can reach dozens of meters if the chipless system cannot be modeled as a linear time-invariant system.

This result can only be achieved by two methods. The first one is by adding a non-linear element to the chipless tag (such as a Schottky diode) to generate a power at multiples of the fundamental frequency. Note that this process is, at that time, not compatible with classical printing technologies. The second method is by breaking the invariance property to generate a power around the carrier frequency (by modulating the backscattered signal as in UHF RFID). For chipless tags, this method requires an external action to modify the tag response in the time domain such as displacement or rotation. In both cases, these transponders are significantly different than the original chipless paradigm.

## VI. Conclusion

This paper highlights the difference between classical RFID (passive and semi-passive) and chipless RFID in term read

range. Also, a new bound for chipless systems in real environment based on the concept of residual environment is introduced. This bound does not depends on the transmitted power nor the reader sensitivity and can not be significantly increased using signal processing techniques. Moreover, the residual environment has been estimated in different configurations (polarization, environment and post-processing techniques). We show that the proposed bound can accurately predict the read range of a chipless system where difference between theoretical read range and the measured one is only 20 cm.

## REFERENCES


[1] R. Harrington, "Electromagnetic scattering by antennas," *IEEE Trans. Antennas Propag.*, vol. 11, no. 5, pp. 595–596, Sep. 1963.

[2] U. Karthaus and M. Fischer, "Fully integrated passive UHF RFID transponder IC with 16.7-μW minimum RF input power," *IEEE J. Solid-State Circuits*, vol. 38, no. 10, pp. 1602–1608, Oct. 2003.

[3] K. V. S. Rao, P. V. Nikitin, and S. F. Lam, "Antenna design for UHF RFID tags: a review and a practical application," *IEEE Trans. Antennas Propag.*, vol. 53, no. 12, pp. 3870–3876, Dec. 2005.

[4] R. R. Fletcher, "Low-cost electromagnetic tagging: design and implementation," Ph.D. dissertation, Massachusetts Institute of Technology, 2002.

[5] I. Jalaly and I. D. Robertson, "Capacitively-tuned split microstrip resonators for RFID barcodes," in *2005 European Microwave Conference*, vol. 2, Paris, France, Oct. 2005, pp. 1–4.

[6] S. Preradovic, I. Balbin, N. C. Karmakar, and G. F. Swiegers, "Multiresonator-based chipless RFID system for low-cost item tracking," *IEEE Trans. Microw. Theory Techn.*, vol. 57, no. 5, pp. 1411–1419, May 2009.

[7] A. Vena, E. Perret, and S. Tedjni, "A depolarizing chipless RFID tag for robust detection and its FCC compliant UWB reading system," *IEEE Trans. Microw. Theory Techn.*, vol. 61, no. 8, pp. 2982–2994, Aug. 2013.

[8] H. T. Friis, "A note on a simple transmission formula," *Proceedings of the IRE*, vol. 34, no. 5, pp. 254–256, May 1946.

[9] P. V. Nikitin and K. V. S. Rao, "Theory and measurement of backscattering from RFID tags," *IEEE Antennas Propag. Mag.*, vol. 48, no. 6, pp. 212–218, Dec. 2006.

[10] P. V. Nikitin, K. V. S. Rao, and S. Lazar, "An overview of near field UHF RFID," in *2007 IEEE International Conference on RFID*, Grapevine, TX, Mar. 2007, pp. 167–174.

[11] A. Abdelnour, A. Hallet, S. B. Dkhil, P. Pierron, D. Kaddour, and S. Tedjini, "Energy harvesting based on printed organic photovoltaic cells for RFID applications," in *2019 IEEE International Conference on RFID Technology and Applications (RFID-TA)*, Pisa, Italy, Sep. 2019, pp. 110–112.

[12] A. P. Sample, D. J. Yeager, P. S. Powledge, and J. R. Smith, "Design of a passively-powered, programmable sensing platform for UHF RFID systems," in *2007 IEEE International Conference on RFID*, Grapevine, TX, Mar. 2007, pp. 149–156.

[13] S. Thomas, J. Teizer, and M. Reynolds, "Smarthat: A battery-free worker safety device employing passive UHF RFID technology," in *2011 IEEE International Conference on RFID*, Orlando, FL, Apr. 2011, pp. 85–90.

[14] A. Sharma, A. T. Hoang, F. Nekoogar, F. U. Dowla, and M. S. Reynolds, "An electrically small, 16.7 m range, ISO18000-6c UHF RFID tag for industrial radiation sources," *IEEE RFID J.*, vol. 2, no. 2, pp. 49–54, Jun. 2018.

[15] T. H. Li, A. Borisenko, and M. Bolic, "Open platform semi-passive RFID tag," in *11th International Conference, ADHOC-NOW 2012*, Belgrade, Serbia, Jul. 2012, pp. 249–259.

[16] S. J. Thomas and M. S. Reynolds, "A 96 Mbit/sec, 15.5 pJ/bit 16-QAM modulator for UHF backscatter communication," in *2012 IEEE International Conference on RFID (RFID)*, Orlando, FL, Apr. 2012, pp. 185–190.

[17] D. De Donno, L. Catarinucci, and L. Tarricone, "A battery-assisted sensor-enhanced RFID tag enabling heterogeneous wireless sensor networks," *IEEE Sensors J.*, vol. 14, no. 4, pp. 1048–1055, Apr. 2014.

[18] V. Pillai, H. Heinrich, D. Dieska, P. V. Nikitin, R. Martinez, and K. V. S. Rao, "An ultra-low-power long range battery/passive RFID tag for UHF and microwave bands with a current consumption of 700 nA at 1.5 V," *IEEE Trans. Circuits Syst. I*, vol. 54, no. 7, pp. 1500–1512, Jul. 2007.

[19] H. El Matbouly, S. Tedjini, K. Zannas, and Y. Duroc, "Chipless sensing system compliant with the standard radio frequency regulations," *IEEE RFID J.*, vol. 3, no. 2, pp. 83–90, Jun. 2019.

[20] M. Garbati, R. Siragusa, E. Perret, A. Vena, and C. Halopé, "High performance chipless RFID reader based on IR-UWB technology," in *2015 9th European Conference on Antennas and Propagation (EuCAP)*, Lisbon, Portugal, Apr. 2015, pp. 1–5.

[21] R. Tavares de Alencar, N. Barbot, M. Garbati, and E. Perret, "Practical comparison of decoding methods for chipless RFID system in real environment," in *2019 IEEE International Conference on RFID Technology and Applications (RFID-TA)*, Pisa, Italy, Sep. 2019, pp. 207–211.

[22] A. Vena, E. Perret, and S. Tedjini, "Chipless RFID tag using hybrid coding technique," *IEEE Trans. Microw. Theory Techn.*, vol. 59, no. 12, pp. 3356–3364, Dec. 2011.

[23] F. Costa, S. Genovesi, and A. Monorchio, "A chipless RFID based on multiresonant high-impedance surfaces," *IEEE Trans. Microw. Theory Techn.*, vol. 61, no. 1, pp. 146–153, Jan. 2013.

[24] M. Khaliel, A. El-Awamry, A. Fawky, and T. Kaiser, "Long reading range chipless RFID system based on reflectarray antennas," in *2017 11th European Conference on Antennas and Propagation (EUCAP)*, Paris, France, Mar. 2017, pp. 3384–3388.

[25] J. G. D. Hester and M. M. Tentzeris, "Inkjet-printed Van-Atta reflectarray sensors: A new paradigm for long-range chipless low cost ubiquitous smart skin sensors of the internet of things," in *2016 IEEE MTT-S International Microwave Symposium (IMS)*, San Francisco CA, May 2016, pp. 1–4.

[26] F. Babaeian and N. C. Karmakar, "A high gain dual polarized ultra-wideband array of antenna for chipless RFID applications," *IEEE Access*, vol. 6, pp. 73 702–73 712, Dec. 2018.

[27] J. G. D. Hester and M. M. Tentzeris, "Inkjet-printed flexible mm-wave Van-Atta reflectarrays: A solution for ultralong-range dense multitag and multisensing chipless RFID implementations for IoT smart skins," *IEEE Trans. Microw. Theory Techn.*, vol. 64, no. 12, pp. 4763–4773, Dec. 2016.

[28] D. Henry, J. G. D. Hester, H. Aubert, P. Pons, and M. M. Tentzeris, "Long range wireless interrogation of passive humidity sensors using Van-Atta cross-polarization effect and 3D beam scanning analysis," in *2017 IEEE MTT-S International Microwave Symposium (IMS)*, Honolulu, HI, Jun. 2017, pp. 816–819.

[29] ——, "Long-range wireless interrogation of passive humidity sensors using Van-Atta cross-polarization effect and different beam scanning techniques," *IEEE Trans. Microw. Theory Techn.*, vol. 65, no. 12, pp. 5345–5354, Nov. 2017.

[30] A. Vena, E. Perret, B. Sorli, and S. Tedjini, "Theoretical study on detection distance for chipless RFID systems according to transmit power regulation standards," in *2015 9th European Conference on Antennas and Propagation (EuCAP)*, Lisbon, Portugal, Apr. 2015, pp. 1–4.

[31] R. Koswatta and N. C. Karmakar, "Investigation into antenna performance on read range improvement of chipless RFID tag reader," in *2010 Asia-Pacific Microwave Conference*, Yokohama, Japan, Dec. 2010, pp. 1300–1303.

[32] R. Anee and N. C. Karmakar, "Chipless RFID tag localization," *IEEE Trans. Microw. Theory Techn.*, vol. 61, no. 11, pp. 4008–4017, Nov. 2013.

[33] ISO/IEC 18000-6:2004 Information technology – Radio frequency identification for item management – Part 6: Parameters for air interface communications at 860 MHz to 960 MHz.

[34] J. G. Proakis and M. Salehi, *Digital communications*. McGraw-Hill, 2001.

[35] M. Hecht and A. Guida, "Delay modulation," *Proceedings of the IEEE*, vol. 57, no. 7, pp. 1314–1316, Jul. 1969.

[36] R. H. Morelos-Zaragoza, "Power spectral densities of baseband signals in EPC Class-1 Gen-2 UHF RFID systems," *San Jose State University*, 2012.

[37] N. Barbot, O. Rance, and E. Perret, "Differential RCS of modulated tag," *IEEE Trans. Antennas Propag.*, in press.

[38] P. V. Nikitin and K. V. S. Rao, "Antennas and propagation in UHF RFID systems," in *2008 IEEE International Conference on RFID*, Las Vegas, NV, Apr. 2008, pp. 277–288.

[39] P. V. Nikitin, K. V. S. Rao, and R. D. Martinez, "Differential RCS of RFID tag," *Electron. Lett.*, vol. 43, no. 8, pp. 431–432, Apr. 2007.

[40] A. Vena, E. Perret, S. Tedjini, G. Eymin Petot Tourtollet, A. Delattre, F. Garet, and Y. Boutant, "Design of chipless RFID tags printed on paper by flexography," *IEEE Trans. Antennas Propag.*, vol. 61, no. 12, pp. 5868–5877, Dec. 2013.